

## Towards regular serendipitous detections of kilonovae by wide-field surveys

MOUZA ALMUALLA,<sup>1</sup> SHREYA ANAND,<sup>2</sup> MICHAEL W. COUGHLIN,<sup>3</sup> TIM DIETRICH,<sup>4</sup> NIDHAL GUESSOUM,<sup>1</sup>  
ANA SAGUÉS CARRACEDO,<sup>5</sup> TOMÁS AHUMADA,<sup>6</sup> IGOR ANDREONI,<sup>2</sup> SARAH ANTIER,<sup>7</sup> ERIC C. BELLM,<sup>8</sup> MATTIA BULLA,<sup>9</sup>  
AND LEO P. SINGER<sup>10,11</sup>

<sup>1</sup>*Department of Physics, American University of Sharjah, PO Box 26666, Sharjah, UAE*

<sup>2</sup>*Division of Physics, Mathematics, and Astronomy, California Institute of Technology, Pasadena, CA 91125, USA*

<sup>3</sup>*School of Physics and Astronomy, University of Minnesota, Minneapolis, Minnesota 55455, USA*

<sup>4</sup>*Institute of Physics and Astronomy, University of Potsdam, Karl-Liebknecht-Str. 24/25, 14476, Potsdam, Germany*

<sup>5</sup>*The Oskar Klein Centre, Department of Physics, Stockholm University, AlbaNova, SE-106 91 Stockholm, Sweden*

<sup>6</sup>*Department of Astronomy, University of Maryland, College Park, MD 20742, USA*

<sup>7</sup>*Université de Paris, CNRS, Astroparticule et Cosmologie, F-75013 Paris, France*

<sup>8</sup>*DIRAC Institute, Department of Astronomy, University of Washington, 3910 15th Avenue NE, Seattle, WA 98195, USA*

<sup>9</sup>*Nordita, KTH Royal Institute of Technology and Stockholm University, Roslagstullsbacken 23, SE-106 91 Stockholm, Sweden*

<sup>10</sup>*Astrophysics Science Division, NASA Goddard Space Flight Center, MC 661, Greenbelt, MD 20771, USA*

<sup>11</sup>*Joint Space-Science Institute, University of Maryland, College Park, MD 20742, USA*

### ABSTRACT

The rise of multi-messenger astronomy has brought with it the need to exploit all available data streams and learn more about the astrophysical objects that fall within its breadth. One possible avenue is the search for serendipitous electromagnetic counterparts of gamma-ray bursts (GRBs) and gravitational-wave signals, known as *kilonovae*. With surveys such as the Zwicky Transient Facility (ZTF), which observes the sky with a cadence of  $\sim$ three days, the existing counterpart locations are likely to be observed; however, due to the significant amount of sky to explore, it is difficult to search for these fast-evolving candidates. It is thus beneficial for the survey cadence to be optimized to find and identify transients of this type such that further photometric and spectroscopic observations can be made. We explore how to improve the cadence of wide field-of-view surveys like ZTF to enable such identifications. We show that with improved observational choices, e.g., the adoption of a  $\sim$ nightly cadence and the prioritization of redder photometric bands, detection rates improve by about a factor of two relative to the nominal cadence. These results demonstrate how an optimal use of ZTF increases the likelihood of kilonova discovery independent of gravitational waves or GRBs, thereby allowing for a sensitive search with less interruption of its nominal cadence through Target of Opportunity programs.

### 1. INTRODUCTION

Large field-of-view all-sky surveys will play a central role in the future of time-domain astronomy. Facilities with survey cadences and fields of view that will enable such endeavors include the Panoramic Survey Telescope and Rapid Response System (Pan-STARRS; Morgan et al. 2012), the Asteroid Terrestrial-impact Last Alert System (ATLAS; Tonry et al. 2018, the Dark Energy Camera (DECam; Flaugher et al. 2015), the Zwicky Transient Facility (ZTF; Bellm et al. 2019a; Graham et al. 2019; Dekany et al. 2020; Masci et al. 2018), and in the near future, BlackGEM (Bloemen et al. 2015) and the Vera C. Rubin Observatory’s Legacy Survey of Space and Time (LSST; Ivezić et al. 2019). The access to recent reference images from these surveys renders the discovery of new transients a routine affair. These facilities employ a variety of follow-up telescopes (e.g. Hook

et al. 2004; Blagorodnova et al. 2018; Wilson et al. 2003; Coughlin et al. 2019b), international consortia of astronomers (e.g. Antier et al. 2020; Gompertz et al. 2020; Lundquist et al. 2019; Kasliwal et al. 2020), image difference pipelines (e.g. Zackay et al. 2016; Becker 2015), and machine learning-based techniques (e.g. Muthukrishna et al. 2019; Ishida et al. 2019) to efficiently follow-up the myriad of transients that are found regularly.

These facilities have had significant success due to serendipitous discoveries of interesting transients, but also play a crucial role in amplifying the returns in the era of multi-messenger astrophysics. Although there have been previous examples of serendipitous detections of short gamma-ray burst (SGRB) afterglows from the intermediate Palomar Transient Factory (iPTF) (Cenno et al. 2015), ATLAS (Stalder et al. 2017), and ZTF (Ho et al. 2020; Kasliwal et al. 2020), the use of space-based gamma-ray observatories to provide localizations

is more common-place. PTF frequently triggered on localizations from the *Fermi* Gamma-Ray Burst Monitor (GBM; Meegan et al. 2009), imaged the region in question, and discovered many GRB afterglows (Singer et al. 2015); ZTF has continued this effort focusing on SGRB afterglows (Coughlin et al. 2019c; Ahumada et al. 2020). These SGRB localizations can span  $\approx 100 - 1000$  square degrees, making their follow-up very challenging for small field of view (FOV) telescopes. Prior to wide-field follow-up of GRBs, the *Swift* mission (Gehrels et al. 2004) was the main discovery engine for afterglows, localizing them with its 1.4 steradian-wide Burst Alert Telescope (BAT) (Barthelmy et al. 2005), X-ray Telescope (XRT) (Burrows et al. 2005), and UV/Optical Telescope (UVOT) (Roming et al. 2005). Due to their rapid evolution from bright to faint luminosities and high to low photon energies, relatively few SGRB afterglows have been identified.

In addition to *Fermi*, there are other instruments actively producing transient alerts with relatively coarse localizations. In particular, these include the Advanced LIGO (Aasi et al. 2015) and Advanced Virgo (Acernese et al. 2015) gravitational-wave (GW) detector network, and IceCube (Aartsen et al. 2017), which detects neutrino events. These localization regions vary from tens to many thousands of square degrees. Generally, because of their scientific importance, these events are followed up as part of Target of Opportunity programs by survey telescopes (e.g. Antier et al. 2020; Gompertz et al. 2020; Lundquist et al. 2019; Kasliwal et al. 2020). Although some of these systems are performing dedicated Target of Opportunity observations of GW, GRB, and neutrino localizations, there are many more transients from the alert generators than cannot be followed up in these modes of operation due to limited telescope time.

Each source type has significantly different lightcurves. GRBs (Klebesadel et al. 1973; Metzger et al. 1997; Gehrels & Mészáros 2012) are traditionally broken up into “short” and “long” (LGRB) classes, although this is subject to debate (Kouveliotou et al. 1993; Norris & Bonnell 2006; Bloom et al. 2008; Zhang & Choi 2008; Bromberg et al. 2013; Zitouni et al. 2015, 2018). In addition to potentially producing SGRBs, compact binary coalescences involving a neutron star also have a broadly isotropic electromagnetic signature known as a *kilonova* (or *macronova*) (Lattimer & Schramm 1974; Li & Paczynski 1998; Metzger et al. 2010; Rosswog 2015; Kasen et al. 2017); see Metzger (2020) for a recent review and further references. This kilonova is driven by the radioactive decay of r-process elements in highly neutron rich, unbound matter that can heat the ejecta

and power a thermal ultraviolet/optical/near-infrared transient. As an exemplary case, after the detection of GW170817 (Abbott et al. 2017), a SGRB afterglow (Alexander et al. 2017; Haggard et al. 2017; Hallinan et al. 2017; Margutti et al. 2017; Troja et al. 2017) and a kilonova counterpart, AT2017gfo (Chornock et al. 2017; Coulter et al. 2017; Cowperthwaite et al. 2017; Drout et al. 2017; Evans et al. 2017; Kasliwal et al. 2017; Kilpatrick et al. 2017; Lipunov et al. 2017; McCully et al. 2017; Nicholl et al. 2017; Shappee et al. 2017; Pian et al. 2017; Smartt et al. 2017; Utsumi et al. 2017) were both discovered.

GW170817 has inspired dedicated searches for serendipitous kilonovae from wide field-of-view surveys, e.g. Pan-STARRS (McBrien et al. 2020) and ZTF (Andreoni et al. 2020a). These analyses, although as yet unsuccessful in detecting strong candidates, are empirically constraining the rates of kilonovae. Serendipitous detections of kilonovae on their own will also enable constraints on the neutron star equation of state (Bauswein et al. 2017; Margalit & Metzger 2017; Coughlin et al. 2019a, 2018a, 2019d; Annala et al. 2018; Most et al. 2018; Radice et al. 2018; Abbott et al. 2018; Lai et al. 2019), the Hubble constant (Coughlin et al. 2020a,b; Abbott et al. 2017; Hotokezaka et al. 2018), and r-process nucleosynthesis (Chornock et al. 2017; Coulter et al. 2017; Cowperthwaite et al. 2017; Pian et al. 2017; Smartt et al. 2017; Watson et al. 2019; Kasliwal et al. 2019).

Recently, following the systematic search for serendipitous kilonovae during the first 23 months of ZTF (described in Andreoni et al. 2020a) a new pipeline for ZTF Realtime Search and Triggering (ZTFReST) has been launched in order to identify kilonova-like transients and rapidly trigger photometric follow-up. This pipeline makes use of techniques such as forced photometry and stacking in order to calculate lightcurve evolution rates that can help distinguish between red, fast-evolving kilonova- and afterglow-like candidates and other kinds of kilonova impostors. Our work complements these significant improvements on kilonova candidate detection pipelines by investigating alternative survey *strategies* that could more efficiently yield kilonovae and multi-messenger counterparts through serendipitous observations.

We describe a path-finder study to improve searches for serendipitous multi-messenger sources with wide field-of-view survey systems, focusing on ZTF. The efficiency of the search for fast transients depends on many factors, including cadence, filter choice, sky coverage, and depth of observations (Andreoni et al. 2019a). We demonstrate that our strategy for survey cadence makes

it possible to detect these sources more efficiently than has been possible until now. Given that the rates and types of background transients are generally known, using ZTF as an example, we can make predictions of the number of transients that will require follow-up to perform characterization and classification. Our paper is structured as follows: we start by describing the scheduling of these observations and their coverage of multi-messenger events in Section 2. The efficiency of counterpart detection for each of these strategies is detailed in Section 3. We summarize our conclusions and future outlook in Section 4.

## 2. SIMULATED OBSERVING PLANS

We aim to determine a survey strategy for ZTF that maximizes the probability of detecting a serendipitous kilonova. During ZTF’s Phase I, which lasted from March 2018 to October 2020, the telescope time was split up between several different programs (Bellm et al. 2019b). Forty percent of the telescope time has been used for public surveys supported by an NSF Mid-Scale Innovations Program (MSIP); another forty percent has been used by the ZTF partnership; and the final twenty percent was disbursed by the Caltech Time Allocation Committee<sup>1</sup>. The largest public survey has been a three-night cadence survey of the Northern Sky. A smaller survey provided one-day cadence monitoring of the Galactic Plane, and latter of the current Northern Hemisphere *TESS* sectors and the current Spektr-RG pointing. Both public surveys obtained one 30-second exposure in both *g*-band and *r*-band every night when a field was observed. The largest partnership program has been an extragalactic transient survey with one day cadence, obtaining six epochs per night split between *g* and *r* filters over a 3000 square degree field at high galactic latitude, resulting in more than 1000 epochs total. The partnership has also conducted a wide *i*-band survey, continuous cadence observations of the Galactic Plane, a twilight survey for asteroids, Target of Opportunity observations, and other specialized programs.

We adopt a simplified scheme in our comparison to ZTF’s Phase I cadence. In ZTF’s Phase II, 50% of the time will be dedicated to an all-sky survey, covering the visible sky every two nights, in 30s exposures. We denote this survey as the “Nominal Survey”. In addition to that program, we will simulate a case by which we use the remaining 50% of the time. Although this is

<sup>1</sup> In ZTF Phase II, fifty percent of the telescope time will be used for public surveys—primarily a two-day cadence survey of the Northern Hemisphere Sky—thirty percent for the ZTF partnership, and twenty percent for the Caltech TAC.

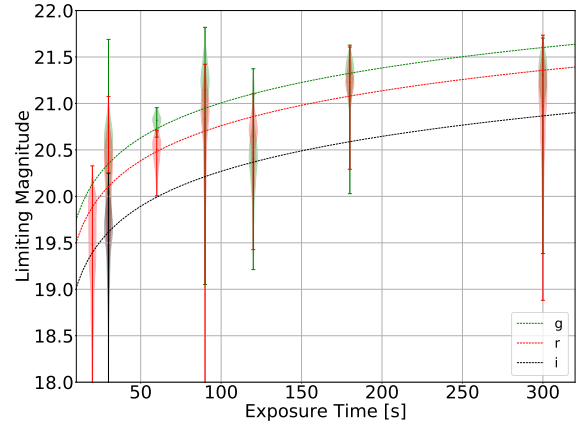


**Figure 1.** Probability density, shown in the form of “violins”, for the limiting magnitudes in *g*-, *r*-, and *i*-bands for the exposure times employed during ZTF Phase I. No conditions have been imposed on factors such as airmass, moon phase, and seeing. Also shown in dashed lines are the expected limiting magnitudes as a function of the median 30s exposures in each passband using the expected  $\sqrt{T}$  scaling (where T is exposure time) appropriate for observations dominated by the sky background.

not completely feasible for a single program, it will nevertheless be informative as scheduling strategies can be adopted to target particular science cases. We denote this survey as the “Kilonova Survey”, during which we also avoid any observations in the galactic plane. In our analysis, we will systematically change the exposure time, the filters, and the cadence in order to optimize observing strategies targeting kilonovae. In essence, the half of the night falling under the Nominal Survey follows the 30s exposure program, with *g*- and *r*-band epochs for each field, while the half that falls under the Kilonova Survey is varied accordingly.

In order to generate realistic schedules to serve as representatives for each strategy, we use `gwemopt` (Coughlin et al. 2018b, 2019e; Almualla et al. 2020), a code-base that was originally designed to perform Target of Opportunity scheduling, but modified here to suit our purposes. Realistic schedules were generated, taking into account factors such as telescope configuration and observational/diurnal constraints. Additionally, in order to generate realistic simulations, the limiting magnitudes in the generated schedules were computed based on past ZTF observations. We show in Figure 1 the limiting magnitudes for *g*-, *r*-, and *i*-bands for the exposure times employed during ZTF Phase I. We also show in dashed lines the expected limiting magnitudes as a function of the median 30s exposures in each passband, using

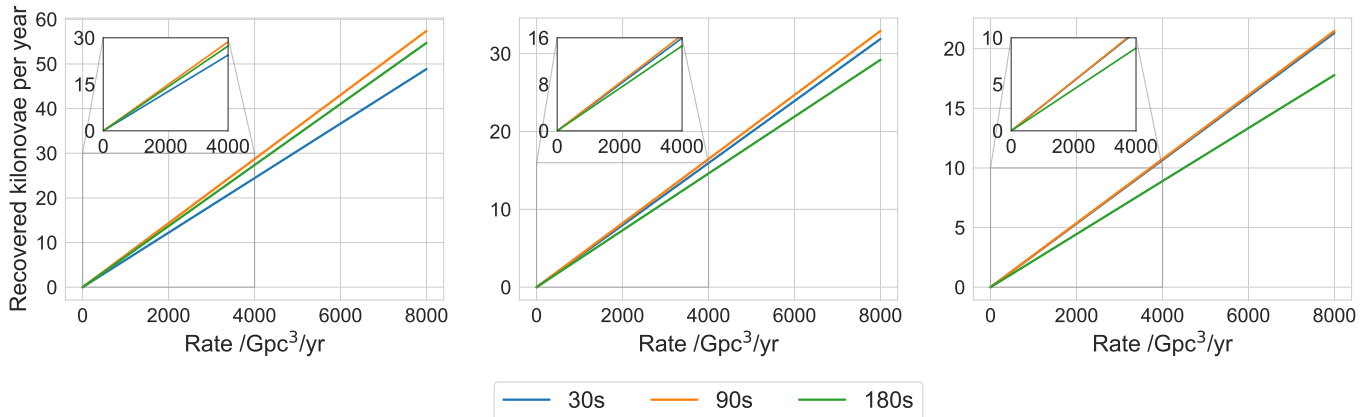


**Figure 2.** Expected number of ZTF kilonova detections per year vs. assumed kilonova rate for the representative 30 s, 90 s, and 180 s schedules, using the GW170817/AT2017gfo-like kilonova model from Bulla (2019). Results are shown for when a one- (left subplot), two- (middle subplot), or three- (right subplot) detection requirement is imposed as part of the filtering criteria. It is clear that the nominal 30 s and the longer 90 s exposure times perform similarly for realistic (two–three) detection requirements, while the 180 s exposures perform more poorly.

the expected  $\sqrt{T}$  scaling appropriate (where  $T$  is exposure time) for observations dominated by the sky background, showing their consistency with the expected evolution. There is some deviation at some points, likely due to the fact that we did not filter for any specific range of factors (e.g., airmass, moon phase, weather conditions), also meaning that there are no biases present in this sense throughout our analysis.

Based on the different elements that constitute the structure of an observing plan (e.g., cadence and filters), we can use different models to assess a given strategy’s performance. In the following, we will use `simsurvey` (Feindt et al. 2019), a software package that simulates the expected lightcurves for the transient. Based on such different factors and setups, we can then determine the possibility of a transient discovery. The models we use when simulating the kilonova population are delineated for each part of our analysis in Section 3.

### 3. RESULTS

#### 3.1. Exposure Time

We first aim to produce an exposure-time optimized strategy, keeping the total time allowed for observations constant so as to fairly evaluate the performance of each plan. We will explore how longer exposure times affect kilonova rate constraints, which can in turn constrain rates of binary neutron star and neutron-star black-hole mergers. There is a natural optimization here, where the longer exposure times achieve more depth, but reduce the number of observations that can be scheduled for the Kilonova Survey, so the interplay between depth achieved and area covered dictates the outcome of this analysis. Here, we focus on 30 s, 90 s, and 180 s exposures. We limit to 180 s exposures, as we found that

longer exposure times do not prove suitable for surveys that aim to cover such large sky areas.

We can first set some rough expectations for the results by approximating the relative “volumes” that each exposure time is sensitive to, assuming a fixed total observing time. From Figure 1, we expect that 30 s exposures will yield a limiting magnitude of  $r \sim 20.1$  mag. Since we are assuming that the sensitivity scales as  $\sqrt{T}$ , the limiting magnitudes for the 90 s and 180 s exposures are  $\sim 20.7$  and  $21.1$  mag respectively. From there, we can compute the approximate sensitive volumes for each of the exposures assuming a transient of  $M_r = -16$  mag (which is approximately the peak absolute magnitude of AT2017gfo in the  $r$ -band). We obtain volumes of 0.019, 0.044, and 0.076  $\text{Gpc}^3$  for 30, 90, and 180 s exposures respectively. Taking into account that ZTF has an overhead of  $\sim 10$  s per exposure, the *total* volume covered by the 30 s exposures for one 90 s exposure is  $\sim 0.048$   $\text{Gpc}^3$ , and 0.090  $\text{Gpc}^3$  for one 180 s exposure. We can see that we are able to cover quite a bit more volume with the 30 s exposures as compared to the one 180 s exposure, but the 90 s exposure actually covers a similar volume to the 30 s exposures. We now compare these expectations to the actual results from `gwemopt` and `simsurvey`, discussed below.

We generate three schedules that adopt 30 s, 90 s, and 180 s exposures respectively for the Kilonova Survey observations. The schedules span one year, covering from 2019-01-01 to 2020-01-01, in order to understand the expected detection prospects over realistic program lengths.

The simulated lightcurves used to calculate efficiencies for this comparison are extracted from a kilonova model with two ejecta mass components (Bulla 2019;

Dietrich et al. 2020); we choose values of  $0.005M_{\odot}$  and  $0.05M_{\odot}$  for the dynamical ( $M_{\text{ej,dyn}}$ ) and post-merger wind ( $M_{\text{ej,pm}}$ ) ejecta masses respectively, and 30 deg for the half-opening angle of the lanthanide-rich component. We assume a uniform viewing angle distribution for the simulated kilonova population. These intrinsic parameters were chosen as a best-fit for the AT2017gfo lightcurve (Dietrich et al. 2020).

The resulting relationship between detections and kilonova rates is shown in Figure 2 for different detection requirements. In practice, fade (or rise) rates, found by performing linear fits before/after the brightest detection, are an essential determinant of whether a detected transient is a possible kilonova (Andreoni et al. 2020b). Therefore, while all cases require further follow-up to confirm kilonovae, the single-epoch case in particular does not provide enough useful information about the nature of the transient. Requiring two to three detections of at least  $5\text{-}\sigma$  is thus standard when filtering transients, making it more likely to identify the expected rapid evolution of kilonovae.

We find that, adopting a one-detection requirement, we can extract slightly tighter constraints (i.e. more stringent upper limits on the rates for a given number of identified kilonovae) from the 90s and 180s observations. If we consider the most recent ZTF rate constraint, assuming a uniform viewing angle distribution, of  $< 4029 \text{ Gpc}^{-3} \text{ y}^{-1}$  (Andreoni et al. 2020b), in the most optimistic scenario, we could expect to discover  $\sim 25$  kilonovae over the year-long survey with the nominal 30s exposures, and  $\sim 29$  kilonovae with the 90s exposures. However, there is little to no improvement for the 90s observations from the nominal exposure time for the two- and three-detection requirements, and the 180s exposures perform more poorly due to the significant loss in sky coverage. For the results above, we computed the observations' limiting magnitudes assuming good seeing conditions (i.e., we only sampled from the past ZTF observations with the top 50% of limiting magnitudes). If we assume more regular seeing conditions (sampling from the entire set of past ZTF observations we have), we nevertheless observe an almost identical trend: 90s and 180s observations perform slightly better for the one-detection requirement, but 90s observations are otherwise on par with the 30s exposures, and the longer 180s observations do not perform as well. Our results are thus consistent with the expectations that were set previously.

This result can contrast with optimal strategies for Target of Opportunity observations of GW and GRB events, for which the areas of interest are constrained to much more reasonable sky localizations; in such cases,

the gain in depth from longer exposure times ( $\gtrsim 180$  s) can usually be exploited without having to worry too much about the loss in coverage (e.g., Ghosh et al. 2017; Coughlin et al. 2020c).

### 3.2. Filters

Although  $g$ - and  $r$ -band observations are useful in identifying the color evolution of transients, the inclusion of  $i$ -band observations has been suggested to be of great benefit for ZTF due to the rapid reddening of kilonovae (Andreoni et al. 2019b; Anand et al. 2020; Carracedo et al. 2020). We therefore generated another year-long schedule, this time implementing three consecutive filter blocks in the  $g$ -,  $r$ - and  $i$ -bands (all of which adopt 90s exposures) for the Kilonova Survey observations. For our analysis, we make use of a more sophisticated linear decay model, adopting a GW170817/AT2017gfo-like evolution. This model is parameterized in terms of  $g$ -band starting absolute magnitude and decay rate (here chosen to be  $M = -16$  mag and  $0.84 \text{ mag day}^{-1}$  respectively), as well as the variables  $\delta M_{g-r}$ ,  $\delta M_{g-i}$ ,  $\delta r_{g-r}$  and  $\delta r_{g-i}$ , which encode the starting  $g-r$  and  $g-i$  colors, and reddening rates in  $r$ - and  $i$ -bands relative to  $g$ -band. We set these parameters such that the decay rates are  $0.68 \text{ mag day}^{-1}$  in  $r$ -band and  $0.45 \text{ mag day}^{-1}$  in  $i$ -band, as measured from our lightcurve fits spanning seven days. We perform similar fits assuming a three-day baseline. Our assumed color evolution is derived from linear fits to the lightcurve and color evolution of GW170817 photometric data (Andreoni et al. 2017; Smartt et al. 2017; Cowperthwaite et al. 2017) in different passbands. By comparing the total number of kilonovae recovered (out of the 10,000 injected) based on their detections in each band, we can then infer the possible benefits of redder  $i$ -band observations.

Since kilonovae fade more slowly in redder bands, the benefit of adopting such a strategy can first be visualized through Figure 3, in which all of the detections in each of the filters are plotted as a function of phase. The  $i$ -band detections extend much further in terms of the time at which the kilonova was detected relative to merger, and so are vital to identifying kilonovae at later times.

More holistically, we can investigate the efficiency of Kilonova recovery in different bands for a number of detection requirements, as shown in Figure 4. We are clearly able to recover a much higher number of kilonovae by including  $i$ -band observations (indicated in black) in addition to those just in  $g$ - and  $r$ -bands (indicated in purple). Here the first three days of evolution are used for the AT2017gfo-like linear decay model, assuming both regular (top subplot) and good (bottom sub-

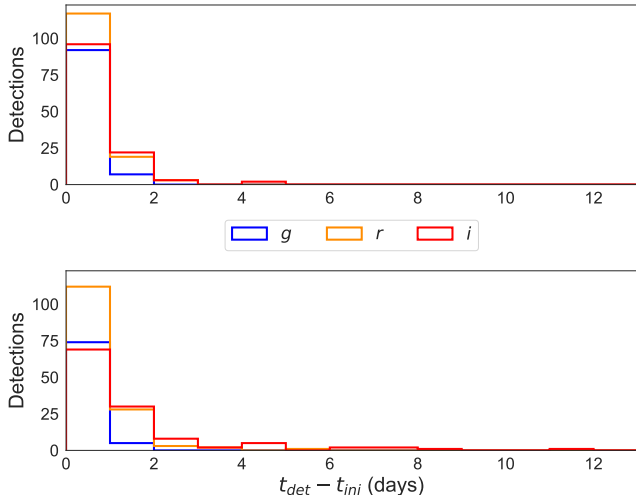


**Figure 3.** Number of detections in  $g$ -,  $r$ -, and  $i$ - bands with respect to the phase of the kilonova at time of detection. Here we show results adopting both a seven-day time window (top) and a three-day time window (bottom) for the AT2017gfo-like linear decay model. Detections in the  $i$ -band start to dominate those in  $g$ - and  $r$ - bands  $\gtrsim 1$  day post-merger in both cases.

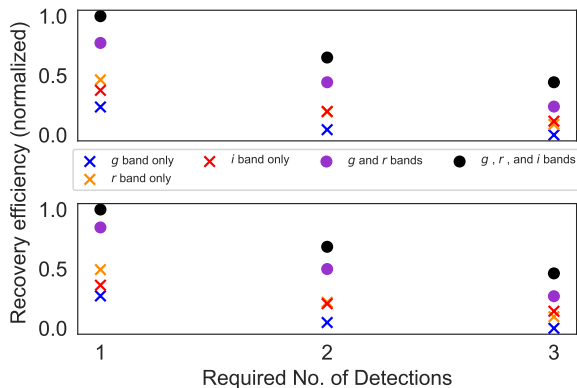


**Figure 4.** A breakdown by filter of the recovered kilonovae for a year-long schedule adopting 90 s  $g$ -,  $r$ -, and  $i$ - band exposures (for the Kilonova Survey); we show results assuming regular conditions (top subplot) and good conditions (bottom subplot). We use the AT2017gfo-like linear decay model, fit to the first three days of evolution, to obtain these efficiencies. The focus here is the improvement when including the  $i$ -band detections (shown in black) as opposed to only those in the  $g$ - and  $r$ -bands (shown in purple).

plot) weather conditions. We find that  $i$ -band observations are especially helpful in poorer conditions, and become more beneficial as the detection requirements become more rigorous. More concretely, we see percent improvements of  $\sim 28\%$ ,  $44\%$ , and  $75\%$  for the one-, two-, and three-detection requirements respectively, from the

recoveries in just  $g$ - and  $r$ - bands. We can also see that, for the three-detection requirement, more kilonovae were recovered with just  $i$ -band detections than there were in just  $g$ -band and just  $r$ -band. Results when fitting our model to the first seven days of evolution are broadly consistent with those shown in Figure 4, leading to increases of  $\sim 34\%$ ,  $55\%$ , and  $66\%$  for each of the one-, two-, and three-detection requirements.

Similar to the results in Section 3.1, the different detection requirements yield different numbers of kilonovae. For example, in the  $g$ -,  $r$ -, and  $i$ -band simulation sets, moving from one detection to two detections loses  $\sim 25\%$  of the recoveries, and one to three detections loses  $\sim 50\%$ .

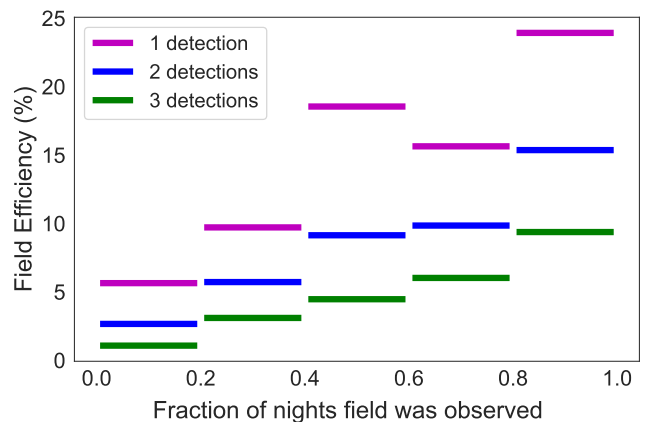


**Figure 5.** Field efficiencies binned by fraction of nights that each of the fields was observed (e.g., a field that was observed every night would correspond to a value of 1.0, and a field observed every other night would correspond to a fraction of 0.5) for one-, two-, and three-detection requirements. We only take into account the 300 s Kilonova Survey observations. For all filtering criteria, there is a clear preference for fields observed at a higher cadence.

### 3.3. Cadence

Aside from exposure times and filters, cadence is another essential determinant of the optimal survey strategy. Naturally, due to the fast-evolving nature of kilonovae, high-cadence strategies are important to optimize their detection with the necessary color and brightness information (see Andreoni et al. 2019b for a more in-depth discussion of cadence-optimized strategies for detecting kilonovae). In order to probe this aspect in a practical manner, we generate a two-week-long 300 s schedule, injecting 10,000 kilonovae into *each field* and computing the per-field efficiencies based on the schedule. We choose 300 s exposures for this part of the analysis because longer exposure times yield much higher percent recoveries in comparison to shorter exposure times

when they are computed on a per-field basis (i.e., total sky area is no longer a factor); this increase leads to less fluctuation in the results, and so helps in isolating cadence from other confounding variables.

We adopt a simple linear decay model defined by a peak absolute magnitude  $M = -16$  mag and a decay rate of  $1.0 \text{ mag day}^{-1}$  in all bands. In Figure 5, we show the field efficiencies binned by the fraction of nights during which they were observed, taking into account Kilonova Survey observations only. There is some fluctuation present in the results, mostly evident for the one-detection requirement; this is likely due to variation in external factors such as the number of epochs scheduled for a field in a given night. In addition, multiple observations within close proximity to each other (on the order of  $\sim$  days) are a less important factor when employing such a lenient filtering requirement.

We can nevertheless see that, for all filtering requirements, there is a positive correlation between the two variables. For the three-detection requirement, for example, the median number of detected kilonovae for fields observed 80-100% of nights, versus that for fields observed 20-40% of nights, increases around fourfold. Since this correlation is strongest for more rigorous detection requirements, higher-cadence strategies will ensure that more potential kilonovae pass all of the filtering criteria. In addition, adopting a high-cadence survey strategy is very useful in ruling out false positives (Mahabal et al. 2019). A nightly cadence or similar is therefore favorable, and facilitates the detection and identification of such fast transients.

#### 4. SUMMARY

In this study, we have presented an overview of how wide field-of-view survey strategies such as those used by ZTF may be used to optimize kilonova searches. We assessed the efficiency of detections emerging from these strategies for a number of models, simulating the potential for serendipitous kilonova discovery in realistic conditions. We demonstrated the significant difference in coverage over these timescales with different exposure times and filter combinations. Finally, we showed how the efficiency of recovery changes as a function of the intra-field cadence.

Having explored the choices that lead to the formulation of the optimal survey strategy in the ZTF search for kilonovae, we may summarize our conclusions as follows:

- **EXPOSURE TIME:** 90 s exposures perform slightly better for a one-detection filtering criterion, but more realistic detection requirements yield similar results for the 30 s and 90 s exposures.

- **FILTERS:** Including *i*-band observations improves the number of recovered kilonovae by up to 75% compared to those recovered in *g*- and *r*-bands only, and is especially useful a few days post-merger.
- **CADENCE:** Adopting a high-cadence strategy (on the order of a nightly, or more frequent, cadence) is essential to maximizing the chances of identifying fast transients.

Although the inclusion of observations in redder filters has been shown to be of benefit in this study, their cadence could possibly be relaxed from the suggested nightly visits due to the longer lasting lightcurve in such bands; this point would be interesting to explore in future studies. We also want to explicitly enumerate some of the simplifications that are likely to affect the results, albeit at a minor level. Our simulations were optimized over 50% of the survey time, although given the other survey priorities such as high-cadence surveys of the Galactic plane, it is likely that this program would receive  $< 50\%$  of the survey time. We also did not take into account that the dome may sometimes be closed due to bad weather; this is not likely to have an effect on our general conclusions, but may lead to an overestimation of the expected number of detections. Throughout, we also assumed only two light curve models resembling the evolution of GW170817, but kilonovae may evolve faster or slower than the rates we assumed. In the case of slower evolution, the detections would still be possible, although for significantly faster evolution, we may miss some of the transients depending on the cadence adopted. We also do not account for efficiency losses due to the image processing pipeline, such as nuclear transients, or the possibility of false positives due to either instrumental effects such as ghosting or astrophysical sources such as cataclysmic variables. In reality, kilonovae detected several days post-peak in redder bands may be more challenging to identify in real-time than projected by our study, due to the relative lack of follow-up imagers with sensitivity in those bands.

Of course, candidate detection with ZTF is not enough to unambiguously identify kilonovae, as we also require follow-up to characterize and classify these sources. This study therefore encourages the need for automated follow-up infrastructure; this includes both infrastructure designed for triggering and collating observations based on external skymaps, such as the GROWTH Target of Opportunity (ToO) marshal (Coughlin et al. 2019c) and the GRANDMA (Global Rapid Advanced Network Devoted to the Multi-messenger Addicts) pipeline (Antier et al. 2019), but also alert stream filtering and marshals such as GROWTH’s marshal

(Kasliwal et al. 2019) and AMPEL (Nordin et al. 2019). In addition, this emphasizes the trend towards singular interfaces to trigger telescope observations, such as the “Target and Observation Managers” (TOMs) being built by Las Cumbres Observatory and others (Street et al. 2018).

Our recommendations overall for redder filters and higher cadence would tremendously benefit ongoing efforts by other groups to identify faint, fast, and red transients with the ZTF survey. Furthermore, this modified strategy will provide us with a much stronger chance of kilonova discovery independent of GWs and GRBs.

We thank Brad Cenko, Mansi Kasliwal, and David Kaplan for the valuable suggestions provided throughout the process of writing this paper. The group at the American University of Sharjah acknowledges a research grant from the Mohammed Bin Rashid Space

Centre (UAE), which supported this work. S. Anand acknowledges support from the GROWTH-PIRE grant 1545949. M. W. Coughlin acknowledges support from the National Science Foundation with grant number PHY-2010970.

Based on observations obtained with the Samuel Oschin Telescope 48-inch and the 60-inch Telescope at the Palomar Observatory as part of the Zwicky Transient Facility project. ZTF is supported by the National Science Foundation under Grant No. AST-1440341 and a collaboration including Caltech, IPAC, the Weizmann Institute for Science, the Oskar Klein Center at Stockholm University, the University of Maryland, the University of Washington (UW), Deutsches Elektronen-Synchrotron and Humboldt University, Los Alamos National Laboratories, the TANGO Consortium of Taiwan, the University of Wisconsin at Milwaukee, and Lawrence Berkeley National Laboratories. Operations are conducted by Caltech Optical Observatories, IPAC, and UW.

## REFERENCES

- Aartsen, M., Ackermann, M., Adams, J., et al. 2017, *Journal of Instrumentation*, 12, P03012–P03012. <http://dx.doi.org/10.1088/1748-0221/12/03/P03012>
- Aasi et al. 2015, *Classical and Quantum Gravity*, 32, 074001
- Abbott, B. P., Abbott, R., Abbott, T. D., et al. 2018, *Phys. Rev. Lett.*, 121, 161101. <https://link.aps.org/doi/10.1103/PhysRevLett.121.161101>
- Abbott, B. P., Abbott, R., Abbott, T. D., et al. 2017, *Nature*, 551, 85
- Abbott et al. 2017, *Phys. Rev. Lett.*, 119, 161101. <https://link.aps.org/doi/10.1103/PhysRevLett.119.161101>
- Acernese et al. 2015, *Classical and Quantum Gravity*, 32, 024001
- Ahumada et al. 2020, To be submitted
- Alexander, K. D., Berger, E., Fong, W., et al. 2017, *ApJL*, 848, L21
- Almualla, M., Coughlin, M. W., Anand, S., et al. 2020, *Mon. Not. R. Astron. Soc.*, 495, 4366. <https://doi.org/10.1093/mnras/staa1498>
- Anand, A., Coughlin, M., & et al. 2020, *Nature Astronomy*
- Andreoni, I., Ackley, K., Cooke, J., et al. 2017, *PASA*, 34, e069
- Andreoni, I., Cooke, J., Webb, S., et al. 2019a, *Monthly Notices of the Royal Astronomical Society*, 491, 5852–5866. <http://dx.doi.org/10.1093/mnras/stz3381>
- Andreoni, I., Anand, S., Bianco, F. B., et al. 2019b, *Publications of the Astronomical Society of the Pacific*, 131, 068004. <http://dx.doi.org/10.1088/1538-3873/ab1531>
- Andreoni, I., Kool, E. C., Carracedo, A. S., et al. 2020a, *Constraining the Kilonova Rate with Zwicky Transient Facility Searches Independent of Gravitational Wave and Short Gamma-ray Burst Triggers*, , , arXiv:2008.00008
- . 2020b, arXiv, arXiv:2008.00008
- Annala, E., Gorda, T., Kurkela, A., & Vuorinen, A. 2018, *Phys. Rev. Lett.*, 120, 172703. <https://link.aps.org/doi/10.1103/PhysRevLett.120.172703>
- Antier, S., Agayeva, S., Aivazyan, V., et al. 2019, *Monthly Notices of the Royal Astronomical Society*, 492, 3904. <https://doi.org/10.1093/mnras/stz3142>
- Antier, S., Agayeva, S., Almualla, M., et al. 2020, *Monthly Notices of the Royal Astronomical Society*, 497, 5518. <https://doi.org/10.1093/mnras/staa1846>
- Barthelmy et al. 2005, *Space Science Reviews*, 120, 143
- Bauswein et al. 2017, *The Astrophysical Journal Letters*, 850, L34. <http://stacks.iop.org/2041-8205/850/i=2/a=L34>
- Becker, A. 2015, *Astrophysics Source Code Library*
- Bellm, E. C., Kulkarni, S. R., Graham, M. J., et al. 2019a, *PASP*, 131, 018002
- Bellm, E. C., Kulkarni, S. R., Barlow, T., et al. 2019b, *PASP*, 131, 068003



- Blagorodnova, N., Neill, J. D., Walters, R., et al. 2018, *Pub. Astron. Soc. Pac.*, 130, 035003
- Bloemen, S., Groot, P., Nelemans, G., & Klein-Wolt, M. 2015, in *Astronomical Society of the Pacific Conference Series*, Vol. 496, *Living Together: Planets, Host Stars and Binaries*, ed. S. M. Rucinski, G. Torres, & M. Zejda, 254
- Bloom, J. S., Butler, N. R., Perley, D. A., et al. 2008, *AIP Conference Proceedings*, doi:10.1063/1.2943423. <http://dx.doi.org/10.1063/1.2943423>
- Bromberg, O., Nakar, E., Piran, T., & Sari, R. 2013, *The Astrophysical Journal*, 764, 179. <http://stacks.iop.org/0004-637X/764/i=2/a=179>
- Bulla, M. 2019, *MNRAS*, 489, 5037
- Burrows et al. 2005, *Space Science Reviews*, 120, 165
- Carracedo, A. S., Bulla, M., Feindt, U., & Goobar, A. 2020, *arXiv*, arXiv:2004.06137
- Cenko et al. 2015, *The Astrophysical Journal Letters*, 803, L24. <http://stacks.iop.org/2041-8205/803/i=2/a=L24>
- Chornock et al. 2017, *The Astrophysical Journal Letters*, 848, L19. <http://stacks.iop.org/2041-8205/848/i=2/a=L19>
- Coughlin, M. W., Dietrich, T., Margalit, B., & Metzger, B. D. 2019a, *Monthly Notices of the Royal Astronomical Society: Letters*, 489, L91. <https://doi.org/10.1093/mnras/513/3>
- Coughlin, M. W., Dietrich, T., Doctor, Z., et al. 2018a, *Monthly Notices of the Royal Astronomical Society*, 480, 3871. <http://dx.doi.org/10.1093/mnras/sty2174>
- Coughlin, M. W., Tao, D., Chan, M. L., et al. 2018b, *Monthly Notices of the Royal Astronomical Society*, 478, 692. <http://dx.doi.org/10.1093/mnras/sty1066>
- Coughlin, M. W., Dekany, R. G., Duev, D. A., et al. 2019b, *Monthly Notices of the Royal Astronomical Society*, 485, 1412. <https://doi.org/10.1093/mnras/stz497>
- Coughlin, M. W., Ahumada, T., Cenko, S. B., et al. 2019c, *Publications of the Astronomical Society of the Pacific*, 131, 048001
- Coughlin, M. W., Dietrich, T., Antier, S., et al. 2019d, *Monthly Notices of the Royal Astronomical Society*, 492, 863. <https://doi.org/10.1093/mnras/stz3457>
- Coughlin, M. W., Antier, S., Corre, D., et al. 2019e, *Monthly Notices of the Royal Astronomical Society*, <http://oup.prod.sis.lan/mnras/advance-article-pdf/doi/10.1093/mnras/stz2485/29808472/stz2485.pdf>, stz2485. <https://doi.org/10.1093/mnras/stz2485>
- Coughlin, M. W., Dietrich, T., Heinzel, J., et al. 2020a, *Phys. Rev. Research*, 2, 022006. <https://link.aps.org/doi/10.1103/PhysRevResearch.2.022006>
- Coughlin, M. W., Antier, S., Dietrich, T., et al. 2020b, *Nature Communications*, 11, 4129. <https://doi.org/10.1038/s41467-020-17998-5>
- Coughlin, M. W., Dietrich, T., Antier, S., et al. 2020c, *Monthly Notices of the Royal Astronomical Society*, 497, 1181–1196. <http://dx.doi.org/10.1093/mnras/staa1925>
- Coulter, D. A., Foley, R. J., Kilpatrick, C. D., et al. 2017, *Science*, 358, 1556
- Cowperthwaite, P. S., Berger, E., Villar, V. A., et al. 2017, *ApJL*, 848, L17
- Dekany, R., Smith, R. M., Riddle, R., et al. 2020, *Publications of the Astronomical Society of the Pacific*, 132, 038001. <https://doi.org/10.1088%2F1538-3873%2F132%2F038001>
- Dietrich, T., Coughlin, M. W., Pang, P. T., et al. 2020, *arXiv*:2002.11355
- Drout, M. R., Piro, A. L., Shappee, B. J., et al. 2017, *Science*, 358, 1570
- Evans, P. A., Cenko, S. B., Kennea, J. A., et al. 2017, *Science*, 358, 1565
- Feindt, U., Nordin, J., Rigault, M., et al. 2019, *Journal of Cosmology and Astroparticle Physics*, 2019, 005–005. <http://dx.doi.org/10.1088/1475-7516/2019/10/005>
- Flaugher, B., Diehl, H. T., Honscheid, K., et al. 2015, *The Astronomical Journal*, 150, 150
- Gehrels, N., & Mészáros, P. 2012, *Science*, 337, 932. <http://science.sciencemag.org/content/337/6097/932>
- Gehrels et al. 2004, *ApJ*, 611, 1005
- Ghosh, S., Chatterjee, D., Kaplan, D. L., Brady, P. R., & Sistine, A. V. 2017, *Publications of the Astronomical Society of the Pacific*, 129, 114503. <https://doi.org/10.1088%2F1538-3873%2F129%2F114503>
- Gompertz, B. P., Cutter, R., Steeghs, D., et al. 2020, *Monthly Notices of the Royal Astronomical Society*, 497, 726–738. <http://dx.doi.org/10.1093/mnras/staa1845>
- Graham, M. J., Kulkarni, S. R., Bellm, E. C., et al. 2019, *Publications of the Astronomical Society of the Pacific*, 131, 078001
- Haggard, D., Nynka, M., Ruan, J. J., et al. 2017, *ApJL*, 848, L25
- Hallinan, G., Corsi, A., Mooley, K. P., et al. 2017, *Science*, 358, 1579
- Ho, A. Y. Q., Perley, D. A., Beniamini, P., et al. 2020, *ZTF20aaajnskq (AT2020blt): A Fast Optical Transient at  $z \approx 2.9$  With No Detected Gamma-Ray Burst Counterpart*, , arXiv:2006.10761
- Hook, I., Jørgensen, I., Allington-Smith, J., et al. 2004, *Pub. Astron. Soc. Pac.*, 116, 425
- Hotokezaka, K., Nakar, E., Gottlieb, O., et al. 2018, *arXiv*:1806.10596

- Ishida, E. E. O., et al. 2019, *Montly Notices of the Royal Astronomical Society*, 483, 2
- Ivezić, Ž., Kahn, S. M., Tyson, J. A., et al. 2019, *ApJ*, 873, 111
- Kasen, D., Metzger, B., Barnes, J., Quataert, E., & Ramirez-Ruiz, E. 2017, *Nature*, 551, 80 EP .  
<http://dx.doi.org/10.1038/nature24453>
- Kasliwal, M. M., Kasen, D., Lau, R. M., et al. 2019, *Monthly Notices of the Royal Astronomical Society: Letters*, doi:10.1093/mnrasl/slz007.  
<http://dx.doi.org/10.1093/mnrasl/slz007>
- Kasliwal, M. M., Anand, S., Ahumada, T., et al. 2020, *Kilonova Luminosity Function Constraints based on Zwicky Transient Facility Searches for 13 Neutron Star Mergers*, , , arXiv:2006.11306
- Kasliwal et al. 2017, *Science*, 358, 1559.  
<http://science.sciencemag.org/content/358/6370/1559>
- . 2019, *Publications of the Astronomical Society of the Pacific*, 131, 038003
- Kilpatrick et al. 2017, *Science*, 358, 1583.  
<http://science.sciencemag.org/content/358/6370/1583>
- Klebesadel, R. W., Strong, I. B., & Olson, R. A. 1973, *The Astrophysical Journal Letters*, 182, L85
- Kouveliotou, C., Meegan, C. A., Fishman, G. J., et al. 1993, *ApJL*, 413, L101
- Lai, X., Zhou, E., & Xu, R. 2019, *The European Physical Journal A*, 55, 60.  
<https://doi.org/10.1140/epja/i2019-12720-8>
- Lattimer, J. M., & Schramm, D. N. 1974, *ApJL*, 192, L145
- Li, L.-X., & Paczynski, B. 1998, *The Astrophysical Journal Letters*, 507, L59.  
<http://stacks.iop.org/1538-4357/507/i=1/a=L59>
- Lipunov et al. 2017, *The Astrophysical Journal Letters*, 850, L1. <http://stacks.iop.org/2041-8205/850/i=1/a=L1>
- Lundquist, M. J., Paterson, K., Fong, W., et al. 2019, *The Astrophysical Journal*, 881, L26.  
<http://dx.doi.org/10.3847/2041-8213/ab32f2>
- Mahabal, A., Rebbapragada, U., Walters, R., et al. 2019, *Publications of the Astronomical Society of the Pacific*, 131, 038002
- Margalit, B., & Metzger, B. 2017, *The Astrophysical Journal Letters*, 850, doi:10.3847/2041-8213/aa991c
- Margutti, R., Berger, E., Fong, W., et al. 2017, *ApJL*, 848, L20
- Masci, F. J., Laher, R. R., Rusholme, B., et al. 2018, *Publications of the Astronomical Society of the Pacific*, 131, 018003
- McBrien, O. R., Smartt, S. J., Huber, M. E., et al. 2020, *PS15cey and PS17cke: prospective candidates from the Pan-STARRS Search for Kilonovae*, , , arXiv:2006.10442
- McCully, C., Hiramatsu, D., Howell, D. A., et al. 2017, *ApJL*, 848, L32
- Meegan et al. 2009, *The Astrophysical Journal*, 702, 791.  
<http://stacks.iop.org/0004-637X/702/i=1/a=791>
- Metzger, B. D. 2020, *Living Rev. Rel.*, 23, 1
- Metzger, B. D., Martínez-Pinedo, G., Darbha, S., et al. 2010, *Monthly Notices of the Royal Astronomical Society*, 406, 2650
- Metzger, M., Djorgovski, S., Kulkarni, S., et al. 1997, *Nature*, 387, 878
- Morgan, J. S., Kaiser, N., Moreau, V., Anderson, D., & Burgett, W. 2012, *Proc. SPIE Int. Soc. Opt. Eng.*, 8444, 0H
- Most, E. R., Weih, L. R., Rezzolla, L., & Schaffner-Bielich, J. 2018, *Phys. Rev. Lett.*, 120, 261103. <https://link.aps.org/doi/10.1103/PhysRevLett.120.261103>
- Muthukrishna, D., Narayan, G., Mandel, K. S., Biswas, R., & Hložek, R. 2019, *Publ. Astron. Soc. Pac.*, 131, 118002
- Nicholl et al. 2017, *The Astrophysical Journal Letters*, 848, L18. <http://stacks.iop.org/2041-8205/848/i=2/a=L18>
- Nordin, J., et al. 2019, arXiv:1904.05922
- Norris, J. P., & Bonnell, J. T. 2006, *The Astrophysical Journal*, 643, 266
- Pian, E., D’Avanzo, P., Benetti, S., et al. 2017, *Nature*, 551, 67
- Pian et al. 2017, *Nature*, 551, 67 EP .  
<http://dx.doi.org/10.1038/nature24298>
- Radice, D., Perego, A., Zappa, F., & Bernuzzi, S. 2018, *The Astrophysical Journal Letters*, 852, L29.  
<http://stacks.iop.org/2041-8205/852/i=2/a=L29>
- Roming et al. 2005, *Space Science Reviews*, 120, 95
- Rosswog, S. 2015, *Int. J. Mod. Phys., D24*, 1530012
- Shappee, B. J., Simon, J. D., Drout, M. R., et al. 2017, *Science*, 358, 1574
- Singer et al. 2015, *The Astrophysical Journal*, 806, 52
- Smartt et al. 2017, *Nature*, 551, 75 EP .  
<http://dx.doi.org/10.1038/nature24303>
- Stalder, B., Tonry, J., Smartt, S. J., et al. 2017, *The Astrophysical Journal*, 850, 149.  
<https://doi.org/10.3847%2F1538-4357%2Faa95c1>
- Street, R. A., Bowman, M., Saunders, E. S., & Boroson, T. 2018, in *Software and Cyberinfrastructure for Astronomy V*, ed. J. C. Guzman & J. Ibsen, Vol. 10707, International Society for Optics and Photonics (SPIE), 274 – 284. <https://doi.org/10.1117/12.2312293>
- Tonry, J. L., Denneau, L., Heinze, A. N., et al. 2018, *Publications of the Astronomical Society of the Pacific*, 130, 064505.  
<http://stacks.iop.org/1538-3873/130/i=988/a=064505>

- Troja, E., Piro, L., van Eerten, H., et al. 2017, *Nature*, 551, 71
- Utsumi, Y., Tanaka, M., Tominaga, N., et al. 2017, *PASJ*, 69, 101
- Watson, D., Hansen, C. J., Selsing, J., et al. 2019, *Nature*, 574, 497
- Wilson, J. C., Eikenberry, S. S., Henderson, C. P., et al. 2003, *Society of Photo-Optical Instrumentation Engineers Conference Series*, Vol. 4841, A Wide-Field Infrared Camera for the Palomar 200-inch Telescope, ed. M. Iye & A. F. M. Moorwood, 451–458
- Zackay, B., Ofek, E. O., & Gal-Yam, A. 2016, *The Astrophysical Journal*, 830, 27.  
<http://stacks.iop.org/0004-637X/830/i=1/a=27>
- Zhang, & Choi. 2008, *Astronomy and Astrophysics*, 484, 293. <https://doi.org/10.1051/0004-6361:20079210>
- Zitouni, H., Guessoum, N., AlQassimi, K. M., & Alaryani, O. 2018, *Astrophysics and Space Science*, 363, doi:10.1007/s10509-018-3449-0.  
<http://dx.doi.org/10.1007/s10509-018-3449-0>
- Zitouni, H., Guessoum, N., Azzam, W. J., & Mochkovitch, R. 2015, *Astrophysics and Space Science*, 357, doi:10.1007/s10509-015-2311-x.  
<http://dx.doi.org/10.1007/s10509-015-2311-x>